Science of the Total Environment 651 (2019) 601–613

Contents lists available at ScienceDirect

Science of the Total Environment

journal homepage: www.elsevier.com/locate/scitotenv

A comprehensive city-level GHGs inventory accounting quantitative estimation with an empirical case of Baoding

Can Lu [a], Wei Li [b,c,*]

[a] School of Economics and Management, North China Electric Power University, Hui Long Guan, Chang Ping District, Beijing 102206, China
[b] School of Economics and Management, North China Electric Power University, No.689 Hua Dian Road, Baoding, Hebei 071003, China
[c] Beijing Key Laboratory of New Energy and Low-Carbon Development (North China Electric Power University), Chang Ping District, Beijing 102206, China

HIGHLIGHTS

- GHG emission inventory of Baoding city is compiled for the first time.
- Five subcategories including comprehensive emission sources are identified.
- Key GHGs indicators and emission mitigation strategies are evaluated.
- This study provides referential significance for city-scale inventory accounting.

GRAPHICAL ABSTRACT

ARTICLE INFO

Article history:
Received 23 July 2018
Received in revised form 16 September 2018
Accepted 17 September 2018
Available online 19 September 2018

Editor: Frederic Coulon

Keywords:
Greenhouse gases
Emission inventory
Energy activity
Municipal waste treatment
Uncertainty analysis

ABSTRACT

Cities represent a critical source and primary unit of Greenhouse Gas (GHG) emissions. The accurate emission accounts of cities provide robust and solid data support for further emission analysis as well as the local low-carbon policy making. Restricted by the data and method lacking, there is a relative lag in city-level emission accounts. Thus, this study attempts to build an investigation-based GHG emission inventory framework for cities. We include CO_2, CH_4, N_2O, and SF_6 emissions from five sources: energy activity, industrial processes/product use, agriculture, land use change/forestry, and waste disposal. This study then uses Baoding as a case study to analyse its emission characteristics. Baoding is a low-carbon pilot city in China, which is a core and crucial city in Jing-Jin-Ji area. It is also the origin of the recently established Xiongan New Area, which has great strategic development significance. The results show that energy activity is the highest emission source followed by waste disposal processes in Baoding. Emissions induced by electricity input that brought from other provinces or cities account for another considerable emission proportion as well. Moreover, agricultural activity, which is a pillar industry in Baoding, contributes the most to methane emissions. Several emissions reduction policy recommendations are provided.

* Corresponding author at: School of Economics and Management, North China Electric Power University, No.689 Hua Dian Road, Baoding, Hebei 071003, China.
E-mail address: ncepulw@126.com (W. Li).

https://doi.org/10.1016/j.scitotenv.2018.09.223
0048-9697/

1. Introduction

The fundamental target of the Paris Agreement is to constrain the global temperature increase to well below 2 °C compared with pre-industrial levels and implement further efforts to stipulate this warming within 1.5 °C (UNFCCC, 2018). A mitigation goal calls for the balance between anthropogenic GHGs and the removals in the form of GHG sinks by the second half of the twenty-first century, which could also be called near-zero emissions (Tanaka and O'Neill, 2018). Undertaking the ambitious effort to overcome warming increase and limit GHGs (greenhouse gas emissions) is therefore an essential task for all countries.

As shown by previous studies (IEA, 2018; Olivier et al., 2017), GHGs of China was indicated with a very large increase on 2003–2007 timescales due to a relative higher energy use growth as well as the soaring developed industrialization. China therefore has become the world's largest emitting country by transcending the United States from 2005 thereafter. However, the proportion of GHG increasing rate was shown with a sharply decline in 2008 given the financial crisis. Since then, a faster growth rate was recovering until 2011 in 8.02%, whereas the increasing rate was manifested with a once more decline in 2012, which was caused by the switch from fossil fuels to non-fossil fuels as well as coal consumption to oil and natural gas consumption.

In recent years, the increasing rate of GHGs implied a flatter magnitude growth with 3.93% and 1.23% in 2013 and 2014, respectively. According to the data from the CAIT Climate Data Explorer of World Resources Institute (WRI), China was the top-ranking emitter among more than 170 countries and accounted for 26.83% of global emissions in 2013 (Johannes Friedrich, 2017). It should be emphasized that, China has pursued significant efforts to regulate and limit GHGs towards a green, energy-saving, and low-carbon pathway. The variation rate of GHGs was then declined to negative with −0.61% and −0.15% for 2015 and 2016, respectively. A point worth highlighting is that, GHGs increased again by 1.7% in 2017 because the economy growth was performed with a higher speed of 7%. A similar pattern of variations emerges in the CO_2 emission trend case for the sake of its dominant share in GHGs as Fig.1 shows. The change situations of non-CO_2 emissions including CH_4, N_2O, and F-gases are also implied in Fig.1. Specifically, we explore the concrete constitutions of GHG emission annually within 11-years horizon from 2006 to 2016 in Fig.2. We calculate the average share for each type of greenhouse gases and obtain that CO_2 emission takes account of the principle status with nearly 79% in aggregate GHGs. CH_4, as presented, is the second largest emitting source in total for 13.81%. The two remaining gases are proved to be lesser at low levels in China.

The national GHGs inventory for 1994, which encompasses in initial National Communication on Climate Change (NDRC, 2004), is the first accomplished inventory that complied as national standard levels in China. This inventory is in accordance with the Revised 1996 IPCC Guidelines for National Greenhouse Gas Inventories (Kroeze et al., 1997) and the referenced Good Practice Guidance as well as Uncertainty Management of National Greenhouse Gas Inventories (Penman, 2000). In subsequent years, it has been called for a provincial level based inventory accounting assignment under the recommendations of NDRC. Liaoning, Yunnan, Zhejiang, Shanxi, Tianjin, Guangdong, and Hubei were selected as the provincial inventory accounting pilots. A set of detailed organization for inventory accounting project was herein launched. The inventory compilation in the 2005 case, which organized and prepared over twenty-four provinces and cities, was initiated under the support of China Clean Development Mechanism Fund. Also recognized that, the work project for controlling GHGs during China's 13th Five-Year period, which aims to limit the decrease of carbon intensity to well below 18% above 2015 level upon 2020 and constraint non-CO_2 emissions with an enhanced stipulate manner, was set reduction target for different areas.

City is the critical source and primary unit of GHGs. Limiting city-level emission are necessarily to ensure GHGs reducing to the national target level. A complete GHG inventory could identify distinct trajectories and features of different type of greenhouse gases which generated from various sources. Besides, policy-related insights into feasible yet flexible mitigation countermeasures could be also offered as well on the basis of an explicit inventory. Compiling an integrated city-level GHGs inventory with its consistency data source is therefore essential.

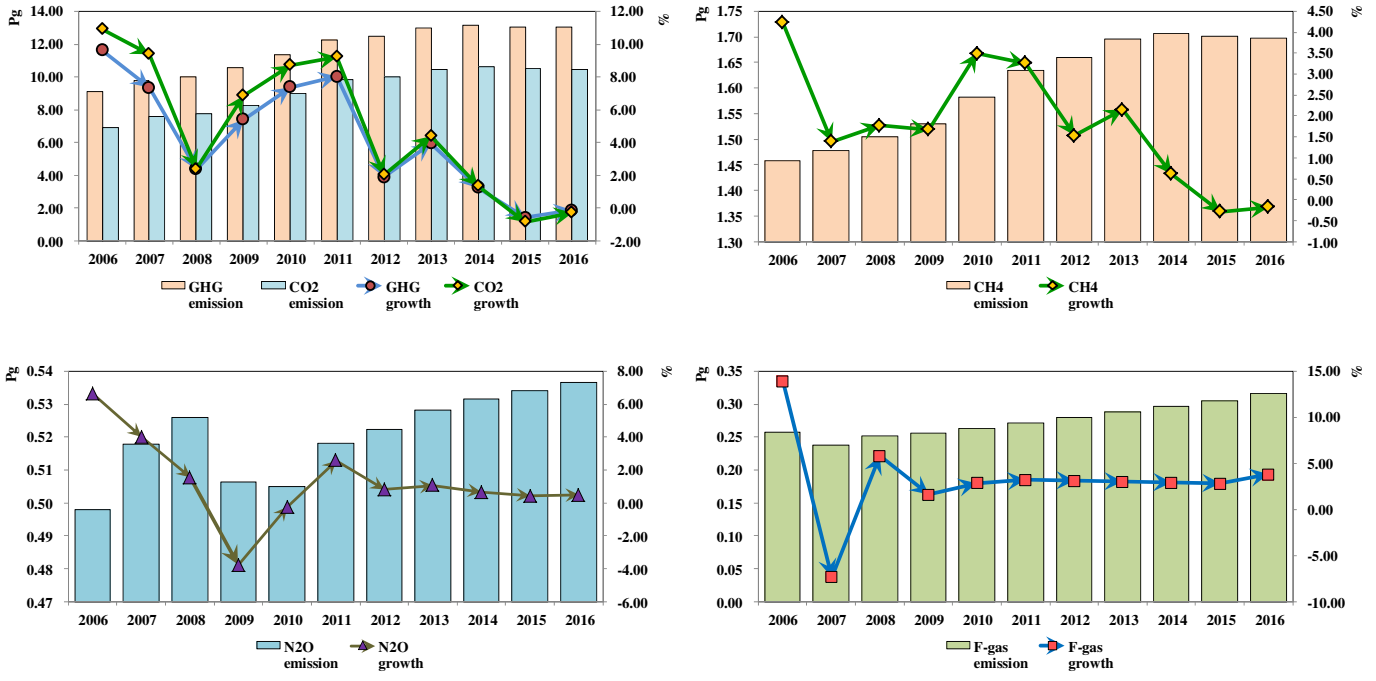

Fig. 1. The variation trend of different greenhouse gases in China.

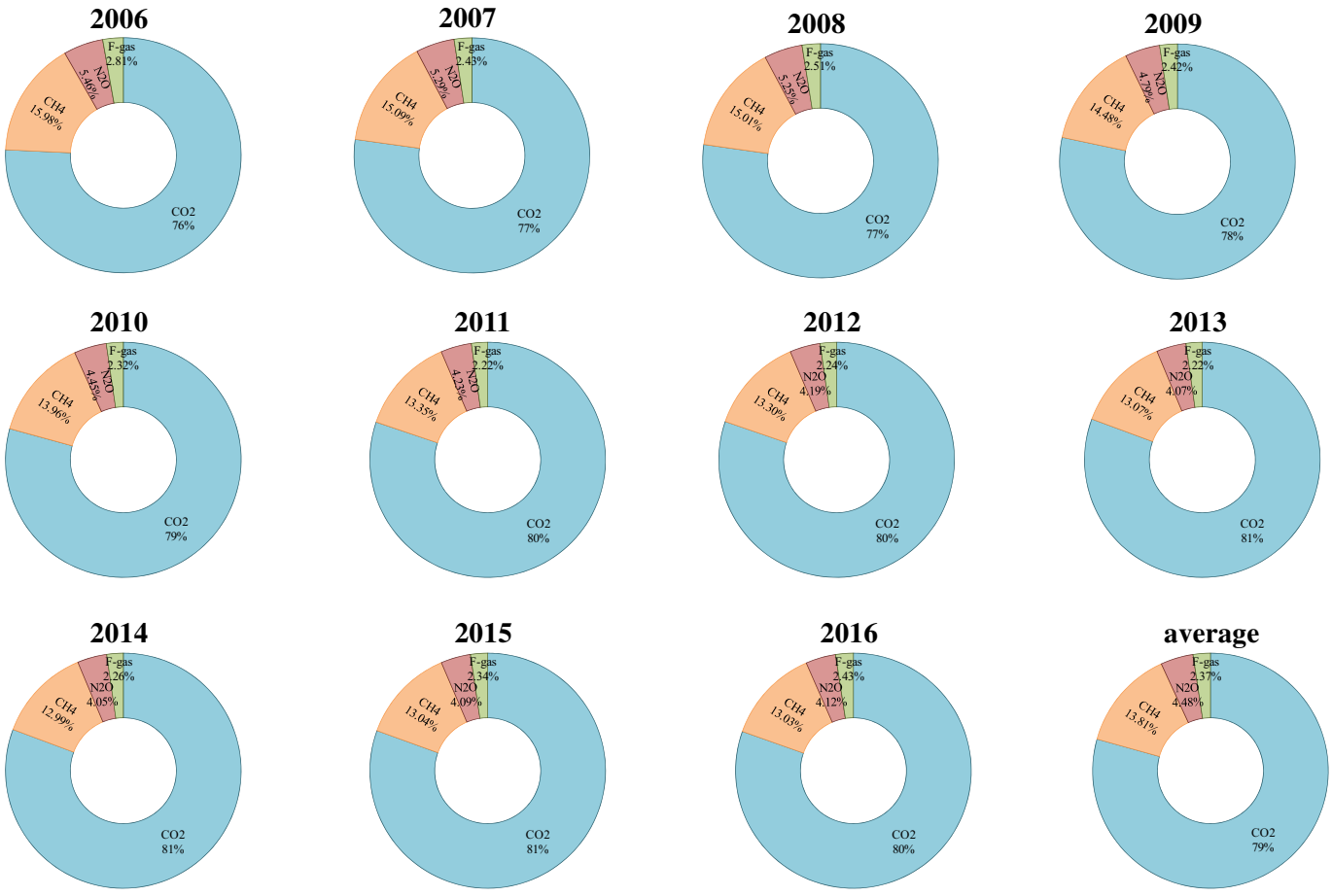

Fig. 2. GHG constitutions during each year in China.

This study addresses three innovations based on the previous city-level GHGs analysis. First, Baoding is chosen as the empirical study case for its significant geographical advantages and instable atrocious air quality disadvantages. It represents the core and crucial region that belonging to the Jing-Jin-Ji area and stands for one of the first batches of low-carbon city pilots in China. Additionally, Xiongan New Area, which would be developed strictly in an ecological, green, and low-carbon pathway, is going independent from Baoding during the first half of 2017. A comprehensive GHG inventory framework research for Baoding is therefore necessary given that very little previous researches have been studied on this city. Regardless of substantial analysis of the city-scale based GHGs methodology has been carried out, nearly no research has modelled GHGs in such a fully and exquisite framework by taking stock of the emission sources exhaustively from five subcategories including energy activity, industrial processes and product use, agriculture activity, land use, land use change and forestry (LULUCF), and waste disposal process in such a third tier Chinese city. Instead, most studies adopted a single method to calculate a single or several sources about GHGs in terms of a single type of greenhouse gas, mostly CO_2 or CH_4. The corresponding method and comparison with previous studies are listed in literature review section. Third, the activity data applied in each subcategory are comparatively true and accurate. The restrict challenge during inventory accounting process, however, is the incomplete statistical data source at the city-level, which is also mentioned in the previous findings (Li et al., 2017; Qi et al., 2018; Xi et al., 2011). Most previous studies extract activity data merely from the existing official statistical documents like statistical yearbook. However, several activity data, which is not compiled in those documents, are indispensable for calculating GHGs and often impose dilemma for researchers. A similar missing data challenge also occurs in our analysis; we therefore carry on a thorough investigation and survey with the contribution of local institutions and related enterprises. The specifically survey procedures can be seen in supplementary materials.

The remaining parts of this paper are organized as follows: Section 2 illustrates the related references and literatures about this issue; the concrete accounting methods of each GHG generating activity are illuminated in Section 3; we put forward the activity data source and emission factors in Section 4; GHG emission results as well as the uncertainty with data or factors are demonstrated in Section 5; this paper finally draws conclusions about GHG emission situations of Baoding and gain insight into policy recommendations in Section 6.

2. Literature review

The current literature of a country-scale (Oehmichen and Thrän, 2017; Villalba and Gemechu, 2011) GHGs inventory mainly focus on two aspects; an interpretation of single pattern emission activity and comparisons with other countries (Abas et al., 2017) or validations from previous study (Talbot and Boiral, 2013). A single activity study, for instance, is mostly concentrated on energy activity (Briones Hidrovo et al., 2017; Cellura et al., 2018; Marchi et al., 2018; Xu et al., 2014) especially transportation energy use emission (La Notte et al.,

2018; Park et al., 2018; Puliafito et al., 2015; Song et al., 2018a; Tayarani et al., 2018) and building energy consumption emission (Wiik et al., 2018), industrial production activity (Hao et al., 2016; Yue et al., 2018), the waste disposal process (Braschel and Posch, 2013; Lou et al., 2017; Song et al., 2018b), and agriculture activity (Baldini et al., 2018; Coderoni and Esposti, 2018).

We arrange the city-scale GHGs inventory analysis into China city-level and foreign country city-level. First, these city-scale GHGs researches based on other countries are shown interest in the pattern of a specific emission from a particular activity or a highlighted sight. Some quintessential cases should be cited that, a city-scale input-output table is applied in Tokyo to assess the energy related carbon emissions. However, non-CO_2 emission was not illuminated in that research (Long and Yoshida, 2018). A simplified GHGs inventory of Sassari was compiled in the context of Global Protocol for Community-Scale Greenhouse Gas Emissions (GPC). Although the integrated inventory was consisted of Stationary Units, Mobile Units, Waste, and Industrial Process and Product Use Emissions, the LULUCF as well as agriculture, remained unaddressed in this study (Sanna et al., 2014). Black carbon emission and the air pollutants like SO2, NOx, CO and NMVOC were calculated together with GHGs inventory of Mezquital Valley using the 1996 IPCC methodology, however, the related activity source were only energy and industrial sectors (Montelongo-Reyes et al., 2015). Similarly, a GHGs inventory analysis only based on the building process was performed at Wroclaw urban area (Sówka and Bezyk, 2018).

Although substantial analysis of city-scale GHGs inventory has been executed in China (Huang et al., 2016; Wang and Liu, 2017; Zeng et al., 2016), most studies has gain insight into how the driving factors affects its levels and which level is more relevant to achieve the reduction or sustainable target, rather than how to contribute endeavour to make the inventory clearly reflect the real emission status. We sort the method of current literature into two aspects. First, a developed framework based on IPCC or other official guidance. One recent case study of Jinan also addresses the GHGs inventory contains these five subcategory activities by implementing life cycle assessment (LCA) with IPCC guidelines to simulate the dynamic changes on 11-year timescales (Qi et al., 2018). However, the limited activity data and emission factors, which were replaced by using the interpolation method and a national level standard (Chinese process-based life cycle inventory database), remain a larger uncertainty. Instead, the method during provincial GHGs inventory guidance, which seems more closely to simulate the local situations, is adopted in our study. Considering the consistency with real conditions, we pursue efforts to increase the accuracy of the activity data by conducting an investigation. As recognized that, the 2014 GHGs inventory following by the framework of the GPC Tool (Li et al., 2017) was made an attempt in the case of Beijing, which is different from the framework IPCCCP in our study. Another similar empirical case is shown in Shenyang with the same framework to compile the GHGs inventory of 2007 (Xi et al., 2011). Second, a specific method deals with a specific issue. As we implied above, the major purpose in the case of Chongqing is exploring the determinants of the dynamic variations of GHGs by carrying out structure decomposition analysis. It is not clear whether the calculation metrics, activity data source, and emission factors were accurate or not (Hu et al., 2017). Similarly, in order to demonstrate the spatial distribution of GHGs with 2005–2010 period horizons, rather than the GHGs inventory accounting description, also occurs in the case of Xiamen (Zhang et al., 2018).

3. Methodology

The complete inventory of GHGs in this study is based on five components: energy activity, industrial processes and production use, agriculture, LULUCF, and waste disposal processes.

3.1. Energy activity

3.1.1. Emission sources

The GHGs from Energy activity is comprised of the related process in energy production, energy transportation, energy conversion, energy combustion and utilization. CO_2, CH_4, and N_2O are the three types of greenhouse gases generated in energy activity. It is shown that mining, petroleum, and natural gas processing activities are not existed in Baoding regardless of 2010 and 2015. Methane fugitive emission from post mineral activity is therefore not considered as well. Consequently, the reporting procedures are mainly focused on three constitutions: Fossil fuel combustion emissions, i.e., CO_2, CH_4, and N_2O; Biomass burning emissions, i.e., CH_4 and N_2O; Indirect carbon emissions arising from electricity input and output.

The fossil fuel combustion emission sources are identified as fossil fuel produced energy use for economic activity and social daily life. This study describes fossil fuel combustion activity from sectoral perspective, technique equipment perspective, and fuel variety perspective. From sectoral perspective, the sectors refer to fossil fuel activity are sorted into six categories with thirteen subdivisions included, which shows in Table S1. From technique equipment perspective, it can also be divided into stationary equipment combustion and mobile equipment combustion, as Table S2 demonstrates. Stationary equipment consists of general equipment, specific equipment, and other equipment. Both electric generation boilers and industrial boilers are belonging to general equipment, whereas blast furnaces, cement kilns, and synthetic ammonia gas furnaces are subordinated to the specific equipment during the iron-steel, building material, and chemical sectors. Alternatively, industrial kilns and heating furnaces are bracketed in the other equipment. From fuel variety perspective, fossil fuel is divided into solid fuel, liquid fuel, and gas fuel. Solid fuel involves with anthracite coal, bituminous coal, lignite coal, cleaned coal, other washing coal, coal products, coal gangue, and coke. Liquid fuel includes crude oil, gasoline, kerosene, diesel oil, fuel oil, liquefied petroleum gas, refinery gas, and other petroleum products. Gas fuel consists of natural gas, coke oven gas, blast furnace gas, converter gas, and other gas.

Biomass fuel combustion indicates straw combustion (fuel-saving stove and traditional stove) and firewood combustion under different equipment levels. Additionally, animal manure and charcoal burning is not included in this study.

Considering the indirect emissions, we also calculate carbon emissions for electricity inputs and outputs in energy activity module.

3.1.2. Methodology

This study uses corresponding methods to estimate CO_2, CH_4, N_2O emissions. Although technology-based sectoral approach is applied in CO_2 emission calculation, however, reference approach is also used to make validations and calibrations focusing on sectoral approach.

The technology-based sectoral approach can be expressed via Eq. (1). Activity data multiplies by emission coefficients for different sectors, equipment, and fuel varieties can be manifested as the core of this method. The consequent carbon emission is the accumulation layer by layer according to the sectoral, equipment, and variety results. In addition, the reference approach is illustrated as Eq. (2).

$$E_{CO2} = \sum\sum\sum\left(EF_{i,j,k} \times Activity_{i,j,k}\right) \quad (1)$$

$$E_{CO2} = (FL \times CC - CS) \times OX \quad (2)$$

Where E_{CO2} represents CO_2 emissions from fossil fuel combustion, $EF_{i,j,k}$ stands for the emission coefficient, and $Activity_{i,j,k}$ shows the activity data, i, j, and k are different sectors, technique equipment, and fuel varieties, respectively. Where FL represents fuel consumption in calorific value units, CC represents per unit heat value of fuel carbon content,

CS represents carbon sequestration, and OX represents the carbon oxidation rate in the combustion process.

The method for N_2O emissions from stationary boilers is similar with Eq. (1). Coal burning consumption from stationary boiler is the activity data. Baoding Quality-Technology Supervision Bureau reveals that oil-fired boilers and gas-fired boilers were not operated from 2010 to 2015. The major boiler type used during this period is the coal-fired vulcanized bed boiler, which primarily consumes anthracite coal and bituminous coal.

N_2O and CH_4 from mobile combustion are merely involved with road transportation emissions, because water transportation and aviation transportation activities are not existed in Baoding. The primary fuels used in road transportation are gasoline and diesel oil. Although the gasoline and diesel oil consumption data from road transportation could not be acquired based on current statistical information, Eq. (3) is applied to calculate N_2O and CH_4 emissions. It is suggested that non-traffic sector accounts for 5% in aggregate mobile fuel combustion. Emissions for N_2O and CH_4 from biofuel combustion can be demonstrated as Eq. (4). Due to the limited official statistical biofuel data sources, basic data with fuel-saving stoves and traditional stoves used by the urban population is adopted.

$$\mathrm{Transport}_{i,j} = \mathrm{Number}_{i,j} \times \mathrm{Mile}_{i,j} \times \mathrm{Oil}_{i,j} \tag{3}$$

$$\mathrm{Biomass}_{i,j} = \mathrm{House}_j/(\mathrm{House}_1 + \mathrm{House}_2) \times \mathrm{StrawFire}_i \tag{4}$$

Where $\mathrm{Transport}_{i,j}$ stands for fuel consumption for road transportation, $\mathrm{Number}_{i,j}$ represents the number of vehicles owned by residents, $\mathrm{Mile}_{i,j}$ indicates the annual length of transport routes, and $\mathrm{Oil}_{i,j}$ is the one-hundred-kilometre oil consumption. Where $\mathrm{Biomass}_{i,j}$ shows the consumption of different types of cookers, House_j defines the numbers of stoves, House_1 illustrates the number of fuel-saving stoves, House_2 demonstrates the number of traditional stove, $\mathrm{StrawFire}_i$ describes straw and firewood combustion, i represents straw and firewood, and j is equal to 1 and 2.

For the sake of no electricity outputs included in the case of Baoding, this study only assesses indirect emissions produced from the electric input, which is equals to the quantity of electricity inputs multiplied by the average power supply factor of the regional power grid.

3.2. Industrial processes and products use

Cement production process, lime production process, iron-steel production process, and electricity equipment production process are the four categories generate CO_2 and SF_6 emissions during industrial processes and product use module.

3.2.1. Emission sources

Carbon emissions produced by the cement production process are mainly come from the intermediate product of cement clinker. The clinker is generated under a series of high-temperature sintering physico-chemical reaction processes for raw meal, as the chemical Eqs. (6)–(7) shows. Subsequently, quick lime (CaO) further reacts with silicon aluminium oxide to form the clinker. Carbon emissions are herein consisted in the process of cement clinker production but not included in the process of carbide slag production. The chemical principle of Carbon emission released from lime production process is the same as Eqs. (6)–(7) shows. The quantity of lime production, which generates $CaCO_3$ and $MgCO_3$, is the determinant of carbon emissions. Two carbon emission sources are observed from iron-steel production process. First, carbon emissions can be generated from ironmaking solvent process under the high-temperature decomposition condition with the similar chemical principle as Eqs. (6)–(7) indicate. Second, the process of lowering carbon content during steelmaking period can also create carbon emissions. Excessive carbon and impurities from pig iron are oxidized by Oxidant under the high temperature condition to formulate carbon emissions or slag. The consumption of limestone and dolomite, the input of pig iron, and the production of steel are therefore required for calculating carbon emissions. Due to the fine insulating property and arc-extinguishing performance of SF_6, it is extensively used in high-voltage switch circuit breakers and gas-insulated electric switchgear production. Therefore, the usage of SF_6 for electricity equipment production process is the emission source.

$$CaCO_3 \rightarrow CaO + CO_2 \tag{6}$$

$$MgCO_3 \rightarrow MgO + CO_2 \tag{7}$$

3.2.2. Methodology

CO_2 emission is proved to be the only type of greenhouse gas released from the cement production process, lime production process, iron-steel production process. We use carbide slag production multiplied by the cement-correlated emission coefficient to calculate carbon emission from cement clinker as Eq. (8) shows. A similar pattern of carbon emission calculation method occurs in the lime production process. Additionally, SF_6 emission is also followed the basic principle of Eq. (8). Where and reflects cement clinker production, lime production, and SF_6 usage; EF_n denotes the corresponding emission coefficients of CO_2 and SF_6. However, carbon emissions produced by iron-steel production process is estimated based on Eq. (9). Where AD_l represents the quantity of limestone used as a solvent in iron-steel enterprises; EF_l and EF_d stand for the corresponding emission factors; AD_d is the quantity of dolomite that used for the solvent; AD_r indicates the amount of pig iron that is used for steel-making; F_r shows the average carbon content of the pig iron used for steel-making; AD_s demonstrates the production of steel; and F_s expresses the average carbon content contained in steel production.

$$E_{CO2} = AD_n \times EF_n \tag{8}$$

$$E_{CO2} = AD_l \times EF_l + AD_d \times EF_d + (AD_r \times F_r - AD_s \times F_s) \times 44/12 \tag{9}$$

3.3. Agriculture activity

The GHGs for agriculture activity contain three constitutions: CH_4 emissions from paddy field and animal intestinal fermentation, N_2O emissions from agriculture land, and CH_4 and N_2O emissions from animal manure management systems.

CH_4 emission source comes from rice field, which can be calculated in line with Eq. (10). Where E_{CH4d} represents the CH_4 emissions from rice field; AD_i shows the sown area of rice; EF_i is the related emission factor; and i indicates the rice categories, including single season rice, double cropping rice, and double season late rice. Only single season rice is planted in the counties of Laishui, Laiyuan, Anxin, Quyang, Shunping due to the location of Baoding. Eq. (10) can also be applied to estimate CH_4 emissions generated from animal intestinal fermentation as well as CH_4 and N_2O emissions produced by animal manure management system; however, the activity data are determined by the numbers of different animals and the corresponding emission factors. CH_4 emission, which generated from animal intestinal fermentation, is determined by the amount of dairy cattle, beef cattle, sheep, goat, pig, horse, donkey, and mule. It should be emphasized that large scale feeding and farmer feeding are preserved but there is no grazing district in Baoding.

N_2O emissions from agriculture land are divided into direct and indirect emissions as shown in Eqs. (11)–(15). Direct emission is caused by seasonal nitrogen inputs to agriculture land, and the input nitrogen contains nitrogenous fertilizer (N_{fer}), manure (N_{man}), and straw incorporation (N_{str}). Indirect emission is caused by N_2O emissions from atmospheric nitrogen deposition ($N_{deposition}$) and nitrogen leaching loss of runoff ($N_{leaching}$), where N_{input} represents the total nitrogen

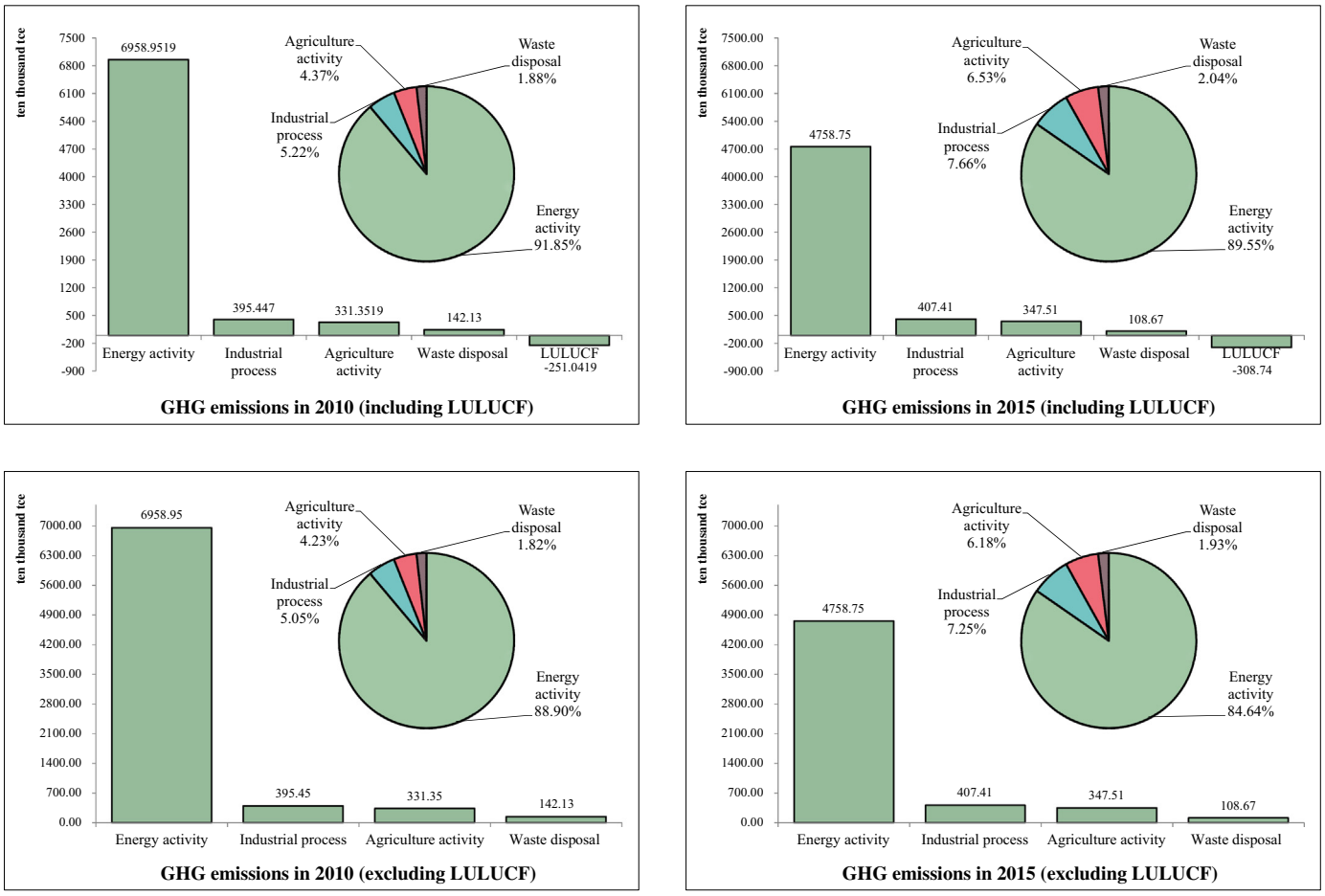

Fig. 3. Total GHG emissions including/excluding LULUCF in 2010 and 2015.

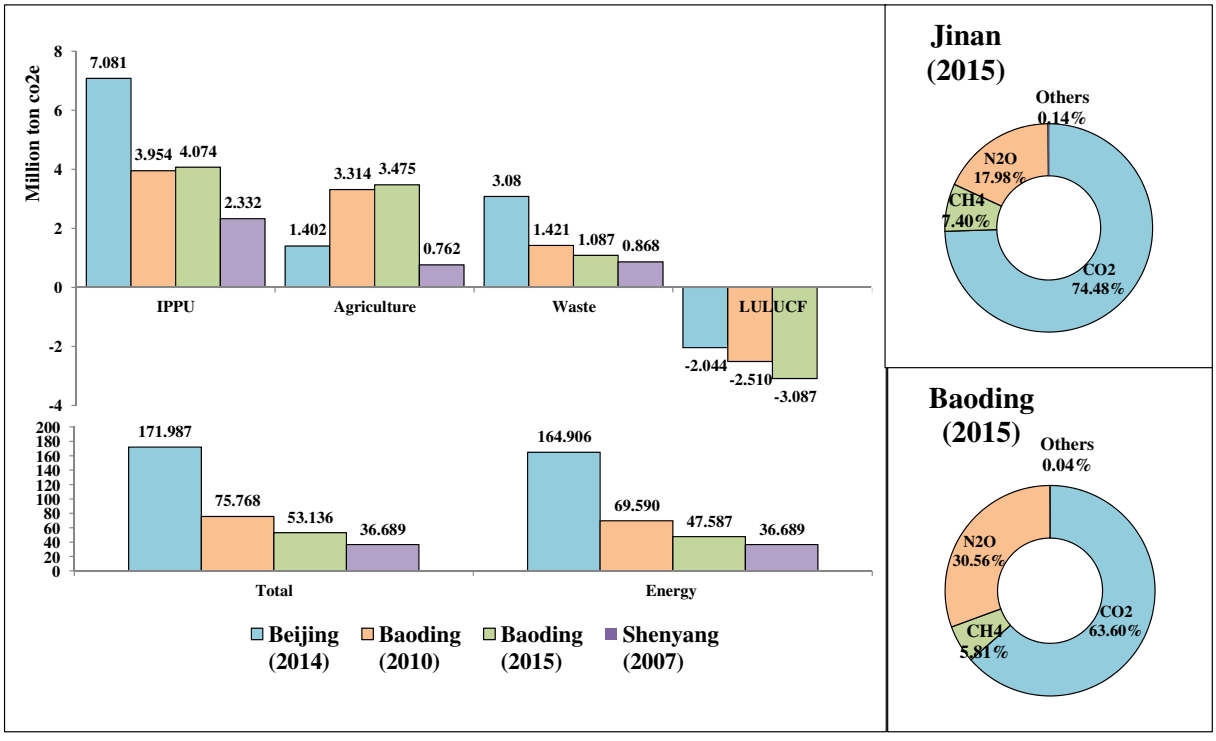

Fig. 4. GHGs comparison with Beijing, Shenyang, and Jinan.

input, N_2O_{direct} stands for the direct N_2O emissions, and $N_2O_{indirect}$ denotes indirect emissions.

$$E_{CH4d} = \sum EF_i \times AD_i \quad (10)$$

$$E_{N2O} = \sum (N_{input} \times EF) \quad (11)$$

$$N_2O_{direct} = (N_{fer} + N_{man} + N_{str}) \times EF_{direct} \quad (12)$$

$$N_2O_{indirect} = N_{deposition} + N_{leachin} \quad (13)$$

$$N_{deposition} = (N_{animal} \times 20\% + N_{input} \times 10\%) \times 0.01 \quad (14)$$

$$N_{leaching} = N_{input} \times 20\% \times 0.0075 \quad (15)$$

3.4. LULUCF

GHG emissions or sinks from LULUCF is mainly depending on changes of biomass carbon storage in forest and other woody biomass as well as carbon emissions from forest transformation.

Changes of biomass carbon storage in forests and other woody biomass ($\Delta C_{biomass}$) involved with three constitutions as Eq. (16) describes. First, biomass carbon absorption leads from the growth of arbour forest (ΔC_{arbour}), scattered wood, four-side trees, and sparse forest (ΔC_{sfp}).

Fig. 5. Different greenhouse gas constitutions.

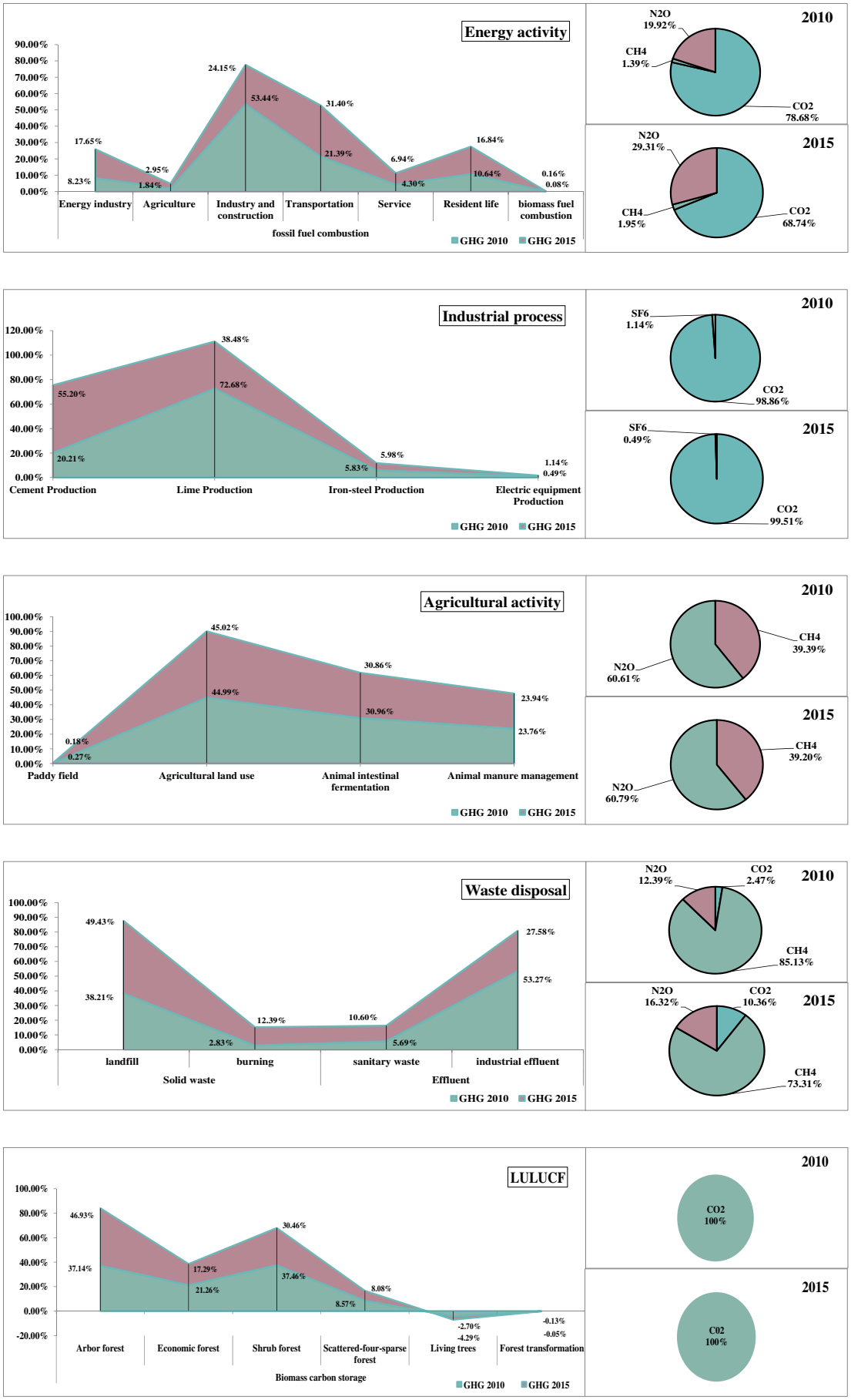

Fig. 6. Different GHGs for five subcategories.

Second, biomass carbon storage changes from bamboo forest, economic forest, and shrub forest (ΔC_{bes}). Third, carbon emissions produced from the consumption of living trees (ΔC_{living}). Carbon absorption from arbor forest growth is shown in Eq. (17). Where V_{arbor} represents the timber volume of arbor forests, GR stands for the annual growth rate of living tree timber volume, $\sum_{i=1}^{n}(SVD_i \cdot \frac{V_i}{V_{arbor}})$ represents the average basic wood density of Baoding, $\sum_{i=1}^{n}(BEF_i \cdot \frac{V_i}{V_{arbor}})$ describes the average biomass conversion coefficient, and V_i reflects the timber volume of different arbor forest species. The estimation of carbon absorption generated from scattered wood, four-side trees, and sparse forest is consistent with Eq. (17). In addition, this study also use Eq. (17) to evaluate carbon emissions from living tree consumption, however we need to substitute GR with the consumption rate of the living tree timber volume CR. Biomass carbon storage changes from bamboo forest, economic forest, and shrub forest can be calculated as Eq. (18). ΔA_{bes} represents the annual area range of bamboo forest, economic forest, and shrub forest, B_{bes} stands for the average unit of biomass area.

$$\Delta C_{biomass} = \Delta C_{arbor} + \Delta C_{sfp} + \Delta C_{bes} - \Delta C_{living} \quad (16)$$

$$\Delta C_{arbour} = V_{arbour} \times GR \times \sum_{i=1}^{n}\left(SVD_i \cdot \frac{V_i}{V_{arbour}}\right) \times \sum_{i=1}^{n}\left(BEF_i \cdot \frac{V_i}{V_{arbour}}\right) \quad (17)$$

$$\Delta C_{bes} = \Delta A_{bes} \times B_{bes} \times 0.5 \quad (18)$$

Carbon emissions generated from forest transformation are primarily from forest burning and forest decomposition. Forest burning consists of burning at local area and other areas. This study only calculate forest burning in other places considering there is no local burning case in Baoding as Eq. (19). Where A represents the annual transformation area, $Biomass_{before}$ and $Biomass_{after}$ reflect the per unit aboveground biomass before and after transformation, $Biomass_{rate}$ defines the burning biomass rate, $Biomass_{oc}$ is the oxidation coefficient, and $Biomass_c$ describes the carbon content of aboveground biomass. Alternatively, Carbon emissions produced by forest decomposition are mainly relied on the surplus biomass slow decomposition process as shown in Eq. (20). Where A_a is the average annual transformation area in ten-year period standards, $Decomp_{rate}$ indicates the proportion rate of forest decomposition.

$$E_{CO2} = A \times (Biomass_{before} - Biomass_{after}) \times Biomass_{rate} \times Biomass_{oc} \times Biomass_c \quad (19)$$

$$E_{CO2} = A_a \times (Biomass_{before} - Biomass_{after}) \times Decomp_{rate} \times Biomass_c \quad (20)$$

3.5. Waste disposal process

Waste disposal process releases CH_4, CO_2, and N_2O. These greenhouse gases are produced by solid waste disposal and effluent disposal. CH_4 emissions and CO_2 emissions are generated from landfill disposal and burning disposal during solid waste disposal process, respectively. Alternatively, CH_4 emissions and N_2O emissions are come from sanitary waste and industrial effluent as well as aggregate effluent during effluent disposal process.

Landfill disposal CH_4 emissions can be assessed in terms of Eqs. (21)–(23). Where MSW_T represents urban solid waste; MSW_F shows the proportion of landfill disposal; L_0 describes the potential of CH_4 emissions in different categories of refuse landfills; MCF demonstrates the corrected CH_4 factors of different categories of refuse landfills; A, B, C stand for the proportion of management degree of different refuse landfills; DOC is the degradable organic carbon; DOC_F indicates the degradable proportion of DOC; F manifests the proportion of CH_4 during various of landfill gas; R expresses the CH_4 recovery; and OX reflects the oxidation factor. Burning disposal waste includes urban solid waste, hazardous waste, and sewage sludge. Eq. (24) is applied to calculate the carbon emissions from burning disposal. Where IW_i represents the scale of burning disposal; CCW_i defines the carbon content proportion of different categories; i is the waste category, involves with urban solid waste, hazardous waste, and sewage sludge; FCF_i implies the mineral carbon proportion over total carbon content for different waste type; and EF_i is the combustion efficiency of the incinerator for the waste type i.

$$EG_{CH4} = (MSW_T \times MSW_F \times L_0 - R)(1 - OX) \quad (21)$$

$$L_0 = MCF \times DOC \times DOC_F \times F \times 16/12 \quad (22)$$

$$MCF = MCF_A \times A + MCF_B \times B + MCF_C \times C \quad (23)$$

$$E_{CO2} = \sum(IW_i \times CCW_i \times FCF_i \times EF_i \times 44/12) \quad (24)$$

CH_4 emissions from sanitary waste and industrial effluent are estimated according to Eqs. (25)–(26), respectively. Where TOW represents the total scale of organic compound, B_O implies the maximum generating capacity of CH_4, and S_i stands for the total scale of organic compound that removed in the form of sludge. N_2O emissions generated from the aggregate effluent can be evaluated in the light of Eq. (27). Where P represents urban population, Pr stands for per capita protein consumption per year, F_{NPR} indicates the nitrogen content of protein, $F_{NON\text{-}CON}$ is the non-depleting protein factors of effluent, $F_{IND\text{-}COM}$ illustrates the protein emission factors of industry and commerce, N_S shows the removed nitrogen accompanied by sludge, and EF_E is the N_2O emission factor.

$$ES_{CH4} = (TOW \times B_O \times MCF) - R \quad (25)$$

$$EGS_{CH4} = \sum[(TOW_i - S_i) \times B_{Oi} \times MCFi) - Ri] \quad (26)$$

$$E_{N2O} = (P \times Pr \times F_{NPR} \times F_{NON\text{-}CON} \times F_{IND\text{-}COM} - N_S) \times EF_E \times 44/28 \quad (27)$$

4. Data source

Table S3 and Table S4 describe the fossil fuel combustion activity data for sectoral approach and reference approach, respectively. Alternatively, the electricity input is 17.1 and 19.064 billion KWH in 2010 and 2015, separately. The activity data of industrial process and product use is shown in Table S6 with an investigation survey on the correlated enterprises. Table S8 represents the consequent activity data for agriculture provided by the economic statistical yearbook and the agricultural bureau. Baoding forest bureau offers the forest resources information and related statistical data for LULUCF as Table S10 illustrates. Additionally, the activity data of waste disposal process, which collected from the environmental statistics of related departments of Baoding, are provided in Table S12.

Based on the 2006 IPCC Guidelines for National Greenhouse Gas Inventories and the National Greenhouse Gas Inventory of People's Republic of China, the corresponding emission factors adopted in this study are shown in Table S5, including the sectoral and reference approach required for the carbon emission coefficients. The emission factors of industrial processes and product use are described in Table S7. The CH_4 and N_2O coefficients from agricultural process are illustrated in Table S9. The emission factors applied to LULUCF are provided in Table S11, and those used in the waste disposal process are shown in Table S13.

Table 1
Inventory results including detailed parts (million tce).

Sources and sinks	CO_2		CH_4		N_2O		SF_6		GHG	
	2010	2015	2010	2015	2010	2015	2010	2015	2010	2015
Total (including LULUCF)	56.276	33.795	3.486	3.085	16.071	16.236	0.045	0.020	75.768	53.136
Energy activity	54.842	32.715	0.971	0.926	13.887	13.946	0	0	69.700	47.587
1. Fossil fuel combustion	54.842	32.715	0.896	0.899	13.852	13.934	0	0	69.590	47.548
Energy industry	5.112	7.737	0	0	0.626	0.661	0	0	5.738	8.398
Agriculture	1.284	1.403	0	0	0	0	0	0	1.284	1.403
Industry and construction	37.248	11.492	0	0	0	0	0	0	37.248	11.492
Transportation	0.785	0.771	0.896	0.899	13.226	13.273	0	0	14.907	14.943
Service	3.000	3.300	0	0	0	0	0	0	3.000	3.300
Resident life	7.413	8.013	0	0	0	0	0	0	7.413	8.013
2. Biomass fuel combustion	0	0	0.075	0.027	0.035	0.012	0	0	0.110	0.039
Industrial process	3.909	4.054	0	0	0	0	0.045	0.020	3.954	4.074
1. Cement production	0.799	2.249	0	0	0	0	0	0	0.799	2.249
2. Lime production	2.874	1.568	0	0	0	0	0	0	2.874	1.568
3. Iron-steel production	0.236	0.238	0	0	0	0	0	0	0.236	0.238
4. Electric equipment	0	0	0	0	0	0	0.045	0.020	0.045	0.020
Agriculture activity	0	0	1.305	1.362	2.008	2.113	0	0	3.314	3.475
1. Paddy field	0	0	0.009	0.006	0	0	0	0	0.009	0.006
2. Agricultural land use	0	0	0	0	1.491	1.565	0	0	1.491	1.565
3. Animal intestinal fermentation	0	0	1.026	1.073	0	0	0	0	1.026	1.073
4. Animal manure management	0	0	0.270	0.284	0.517	0.548	0	0	0.787	0.832
LULUCF	−2.510	−3.087	0	0	0	0	0	0	−2.510	−3.087
1. Biomass carbon storage	−2.514	−3.089	0	0	0	0	0	0	−2.514	−3.089
Arbor forest	−0.932	−1.449	0	0	0	0	0	0	−0.932	−1.449
Economic forest	−0.534	−0.534	0	0	0	0	0	0	−0.534	−0.534
Shrub forest	−0.940	−0.940	0	0	0	0	0	0	−0.940	−0.940
Scattered wood, four-side tree, and sparse forest	−0.215	−0.249	0	0	0	0	0	0	−0.215	−0.249
Living trees' consumption	0.108	0.083	0	0	0	0	0	0	0.108	0.083
2. Forest transformation	0.0032	0.0015	0	0	0	0	0	0	0.003	0.002
Combustion	0.0015	0.0007	0	0	0	0	0	0	0.002	0.001
Decomposition	0.0017	0.0008	0	0	0	0	0	0	0.002	0.001
Waste disposal	0.035	0.113	1.210	0.797	0.176	0.177	0	0	1.421	1.087
1. Solid waste	0.035	0.113	0.476	0.449	0	0	0	0	0.511	0.562
2. Effluent	0	0	0.734	0.347	0.176	0.177	0	0	0.910	0.525
Electricity input (indirect)	21.300	23.740	0	0	0	0	0	0	21.300	23.740

5. Results and discussion

5.1. GHGs constitution analysis

We convert the SF_6, CH_4, N_2O emission into carbon emission equivalents in line with the 100-year global warming potential index. The aggregate GHGs including LULUCF are 75.768 and 53.135 Mt. CO2e in 2010 and 2015, respectively. Specifically, energy activity releases 69.589 and 47.587 Mt. CO_2e in 2010 and 2015, respectively; industrial processes and product use produce 3.954 and 4.074 Mt. CO_2e in 2010 and 2015, respectively; and agriculture activity generates 3.313 and 3.475 Mt. CO_2e in 2010 and 2015, respectively. Moreover, the absorption via LULUCF is 2.51 and 3.087 Mt. CO_2e in 2010 and 2015, respectively. Waste disposal processes generate 1.421 and 1.086 Mt. CO_2e in 2010 and 2015, respectively. Therefore, the aggregate GHGs that do not consist of LULUCF are 78.684 and 56.223 Mt. CO_2e in 2010 and 2015, respectively. A detailed account of each component is shown in Fig. 3.

We have made a contrast between the GHGs results of Baoding and Beijing taking account of the previous studies (Li et al., 2017; Xi et al., 2011), as Fig. 4 shows. The total GHGs of Beijing in 2014 is 1.30 and 2.28 times larger than Baoding in 2010 and 2015 with LULUCF included, respectively. The GHGs produced by agriculture activity in 2014 for Beijing, however, is proved to be lesser than that of Baoding with approximately 60% in both 2010 and 2015. In terms of the similar GHGs calculation framework, this study also compares the results with the case of Shenyang. Conversely, the case for Shenyang in 2007 shows a lower level with respect to Baoding nearly in all the subcategories except the agriculture and LULUCF combination sphere. It is 0.86 and 0.30 times lesser than GHGs for the case of Baoding in 2010 and 2015, separately. Also recognized is that, the GHGs generated from the mixture of agriculture and LULUCF for Shenyang is 0.49 times larger than that of 2015 for the case of Baoding.

From greenhouse gas category perspective, the aggregate carbon emissions are 56.275 and 33.794 Mt. CO_2e; the total emissions of CH_4 are 34.862 and 30.85 Mt. CO_2e, N_2O are 16.07 and 16.236 MtCO_2e and the fluorine-containing gas SF_6 are 0.045 and 0.020 Mt. CO_2e, with LULUCF consisted in the total GHGs in 2010 and 2015, respectively. When LULUCF-based GHGs are not considered, the total carbon emissions for 2010 and 2015 are 58.786 and 36.882 Mt. CO_2e, respectively; and the total CH_4, N_2O, and SF_6 emissions for 2010 and 2015 are

Table 2
PCGHG comparison with other cities (tCO_2e per capita).

Cities	Countries	Study year	Value
Denver	U.S.	2005	25.3
Los Angeles	U.S.	2000	13
Toronto	Canada	2005	11.6
Cape Town	South Africa	2005	11.6
Bangkok	Thailand	2005	10.7
New York	U.S.	2005	10.5
London	U.K.	2003	9.6
Prague	Czech Republic	2005	9.4
Geneva	Switzerland	2005	7.8
Barcelona	Spain	2006	4.2
Baoding	China	2010	6.76
Baoding	China	2015	5.13
Beijing	China	2014	8.10
Jinan	China	2015	9.95
Xiamen	China	2009	5.24
Shenyang	China	2007	8.04

Notes: The source data is mainly collected from studies (Kennedy et al., 2009; Li et al., 2017; Qi et al., 2018; Xi et al., 2011).

Table 3
The data fluctuation range for each part (%).

Sources and Sinks	Standard deviation	
	2010	2015
Energy activity	[6, 7]	[7, 8]
1. Fossil fuel combustion	[6, 7]	[7, 8]
Energy industry	[6, 9]	[6, 9]
Agriculture	[6, 7]	[6, 7]
Industry and construction	[8, 9]	[4, 6]
Transportation	[20, 22]	[23, 25]
Service	[9, 10]	[8, 10]
Resident life	[9, 10]	[8, 10]
2. Biomass fuel combustion	[3, 4]	[3, 5]
Industrial process	[11, 12]	[6, 8]
1. Cement PRODUCTION	[4, 6]	[5, 6]
2. Lime production	[14, 16]	[14, 16]
3. Iron-steel production	[12, 13]	[12, 14]
4. Electric equipment production	[8, 9]	[8, 9]
Agriculture activity	[18, 20]	[14, 16]
1. Paddy field	[43, 45]	[43, 45]
2. Agricultural land use	[23, 25]	[4, 6]
3. Animal intestinal fermentation	[33, 35]	[33, 35]
4. Animal manure management	[47, 49]	[47, 49]
LULUCF	[25, 26]	[25, 27]
1. Biomass carbon storage	[23, 26]	[25, 27]
2. Forest transformation	[23, 26]	[30, 31]
Waste disposal	[20, 22]	[21, 23]
1. Solid waste	[36, 39]	[35, 40]
2. Effluent	[33, 36]	[35, 40]
Electricity input (indirect CO_2)	[5, 7]	[5, 7]

3.486, 1.607, and 0.045 Mt. CO_2e and 3.085, 1.623, and 0.02 Mt. CO_2e, respectively. The corresponding constitution results are manifested in Fig. 5. Fig. 6 demonstrates the detailed proportion for each category. Additionally, this study also contrasts the previous case of Jinan (Qi et al., 2018) with this study in the light of the GHG constitutions. Approximately all the GHGs of Jinan case indicate a relatively larger magnitude with respect to the case of Baoding in 2015 except N_2O emissions. It should be emphasized that N_2O emissions of Jinan implies a lesser trend than that of Baoding. We can infer that the agriculture emission in Baoding is therefore larger than the case of Jinan because approximately the major parts of N_2O emissions are originated from agriculture (Table 1).

5.2. Key indicator analysis

This study selects three key indicators, the carbon emissions per unit gross domestic product (CEPGDP), per capita GHGs (PCGHG), and carbon emissions per unit energy consumption (CEPEC), to observe the variations of GHGs from 2010 to 2015. When LULUCF is included, the CEPGDP is 1.873 tCO_2/thousand USD in 2010 but decreases to 0.729 tCO_2/thousand USD in 2015; the PCGHG is 6.76 tce per capita in 2010 but declines to 5.134 tce per capita in 2015; and the CEPEC is 3.885 tCO_2/tec in 2010 but declines to 2.022 tCO_2/tec in 2015. Different indicator results are observed if LULUCF is not included in the aggregate GHGs: the CEPGDP is 1.957 and 0.796 tCO_2/thousand USD in 2010 and 2015, respectively; the PCGHG is 6.984 and 5.432 tce per capita in 2010 and 2015, respectively; and the CEPEC is 4.059 and 2.206 tCO_2/tec in 2010 and 2015. In contrast, the results of PCGHG values in this study are compared with the different levels of Chinese cities and global cities according to the previous findings as Table 2 shows. Although the PCGHG of each case city might be not extremely similar due to the sample selection and time horizons under different calculation metrics, the basic emission situations could be reflected. Baoding is a medium-level GHG emission city with respect to the listed Chinese cities in the same time points. The maximum PCGHG city is Jinan beyond current cases. We can infer that the European cities like London, Geneva, and Barcelona indicate a relatively lower level in the early periods over 2003–2006. Specifically, the value of PCGHG for Barcelona in 2006 is even 0.18 times lower than that of Baoding in 2015.

Although we calculate total GHGs focusing on five spheres, each sphere is not an independent emission source. This study therefore explores the related reference researches to reveal the interactions between soil characteristic and solid waste management GHGs. One recent study addresses the municipal solid waste (MSW) treatment management option issue by carrying out Life Cycle Carbon Accounting and Carbon Emission Pinch Analysis under different specified carbon emission constraints for the case city of Qingdao. The results show that landfill MSW treatment method is the main management option upon 2020, and waste heat generated during incineration is the most GHGs reduction treatment method during 2020–2035 horizons. A similar MSW treatment pattern of landfill is also occurred in the case of Baoding within the sample period based on the advanced technique limitations, for instance, waste heat generating technology during incineration and CO_2 capture and storage (CCS) technology from MSW incinerations. However, the incineration treatment would be impact on the soil characteristic and might be further affect the carbon sequestration ability from LULUCF. One recent study (Amponsah et al., 2018) has addressed this issue using LCA method and obtained that incineration had the highest mean GHG emissions with 0.7 tCO2-eq/m^3 and thermal desorption show the lowest with 0.07 tCO2-eq/m^3. Alternatively, a case study of Switzerland (Leifeld, 2018) shows that the reliability of organic soil N_2O emissions can be improved by the measurement of soil C/N ratios. Herein, the optimal GHGs reduction strategies should be considered the interactions between emissions by MSW treatment methods and removals by absorptions of LULUCF.

5.3. Uncertainty evaluation

Although we have made considerable efforts to improve the quality and accuracy of the inventory using different methods, such as the investigation and survey based on enterprises and local government bureaus, uncertainty is even unavoidable during the inventory accounting process. The activity data uncertainty is caused by the missing statistical information. For example, annual operation kilometres and oil consumption per 100-kilometres, the usage of SF_6 in the electric equipment production process, and the consumption of limestone and dolomite in the steel production process are lacked. Therefore, the uncertainty fluctuation range for each data source is shown in Table 3.

Table 4
Uncertainty of the inventory (%).

Source	CO_2		CH_4		N_2O		SF_6		Aggregate uncertainty	
	2010	2015	2010	2015	2010	2015	2010	2015	2010	2015
Energy activity	5.96	3.72	19.75	23.01	20.39	22.55	0	0	**6.21**	**7.09**
Industrial process	11.2	6.6	0	0	0	0	8.5	8.5	**11.1**	**6.6**
Agricultural activity	0	0	28.53	28.79	25.21	18.26	0	0	**18.97**	**15.83**
LULUCF	25.56	25.81	0	0	0	0	0	0	**25.56**	**25.81**
Waste disposal	36.40	27.13	24.11	28.32	56.91	56.91	0	0	**21.72**	**22.92**
Aggregate uncertainty	**5.97**	**4.38**	**14.64**	**16.21**	**17.91**	**19.52**	**8.50**	**8.50**	**5.87**	**6.64**

The bold values represent aggregate uncertainty of each subcategory activity and each type of greenhouse gas.

This study uses the error transfer formula to evaluate the uncertainty of the inventory, as shown in Eqs. (28)–(29). Where U_{c1} and U_{c2} represent the uncertainty of the sum or difference and product of the estimation value in a set of n; U_{s1}, ⋯, U_{sn} stands for the uncertainty of the estimation value; and u_{s1}, ⋯, u_{sn} indicates the estimation value. Thus, this study assesses the uncertainty for the five subcategories of GHGs. The uncertainty evaluation results are shown in Table 4.

$$U_{c1} = \frac{\sqrt{(U_{s1}\cdot u_{s1})^2 + (U_{s2}\cdot u_{s2})^2 + \cdots + (U_{sn}\cdot u_{sn})^2}}{|u_{s1} + u_{s2} + \cdots + u_{sn}|} = \frac{\sqrt{\sum_{n=1}^{N}(U_{sn}\cdot u_{sn})^2}}{\left|\sum_{n=1}^{N} u_{sn}\right|} \quad (28)$$

$$U_{c2} = \sqrt{(U_{s1}\cdot u_{s1})^2 + (U_{s2}\cdot u_{s2})^2 + \cdots + (U_{sn}\cdot u_{sn})^2} = \sqrt{\sum_{n=1}^{N}(U_{sn}\cdot u_{sn})^2} \quad (29)$$

6. Conclusions and policy implications

Previous case studies based on city-scales are mainly concentrated on the energy consumption oriented emissions without other greenhouse gases consisted. This study is the first comprehensive GHGs inventory compilation case for the significant city of Baoding in Hebei province that takes approximately the absolute emission sources and sinks into account. Based on the results and discussion presented above, several conclusions and policy recommendations are provided as follows.

First, it is in line with the previous findings that energy activity is the highest emission sources with respect to the other activities. Specifically, the fossil fuel consumption in manufacturing and construction industry accounts for the maximum proportion among other industries. Thus the process of completing traditional manufacturing industry transformation and upgradation should be push forward rapidly to constrain fossil fuel consumption. From construction sector reduction perspective, it is urgent to comprehensively promote green building development schemes and utilize energy-saving construction materials.

Except for this common conclusion, our results also offer a highlighting insight that N_2O emission is proved to be the second highest emission gas contrast with other gases. N_2O emission is mainly released from agriculture and waste disposal process. As seen likely in the statistical information of Baoding, agriculture is one of the pillar industries with a large fraction of paddy fields and other type of grain crops as well as fruits and vegetables focusing on the counties of Mancheng, Yixian, Laiyuan, and Shunping. This paper therefore implies that the agricultural reduction technology, such as nitrogen fertilizer irrigation technology, the direct return of crop stalks, the return of farmland to livestock, the adoption of organic fertilizer and green manure, implementation of organic and inorganic fertilization, should be encouraged. In addition, waste treatment activity accounts for the largest GHGs besides energy activity due to the conventional MSW management means in the form of incineration and landfill without energy recovery and CCS technology. The recycling and reusing utilization of MSW should be developed to promote energy conservations. For instance, landfill gas should be captured and used as fuel to generate electricity and heat to decrease traditional fossil fuel combustion.

Second, it is emphasized that industrial process emission occupies a major proportion in China, however, GHGs from industrial process account for only 6.87% in 2015 for Baoding. We can infer that GHGs produced by industrial process is even lesser in Xiongan new area. Therefore, it has a tremendous superiority and potential for Xiongan new area to develop innovative high-tech and technology-intensive industries.

Third, carbon emission intensity decreases at an annual average rate of 11.46%, GHGs per capita are reduced by 4.2%, and GHGs per unit of energy consumption also decline by 9.59% with 2010–2015 timescales. Correspondingly, the amounts of lime and iron-steel production enterprises have experienced a sharp decline owing to the overcapacity resolving policy guidance. In 2010, the lime and iron-steel production enterprise quantity are approximately 200 and 50, but it was declined to 75 and 1 upon 2015, respectively. This phenomenon implies that dismantling the production capacity of heavy industry is identified as an efficient strategy for reducing GHGs.

Conflicts of interest

The authors declare that there are no conflicts of interest regarding the publication of this paper.

Acknowledgements

This study is supported by the Fundamental Research Funds for the Central Universities (NO. 2018QN094) and the National Social Science Foundation of China (NSSFC) (Grant No. 15BGL145).

Appendix A. Supplementary data

Supplementary data to this article can be found online at https://doi.org/10.1016/j.scitotenv.2018.09.223.

References

Abas, N., Kalair, A., Khan, N., Kalair, A.R., 2017. Review of GHG emissions in Pakistan compared to SAARC countries. Renew. Sust. Energ. Rev. 80, 990–1016.
Amponsah, N.Y., Wang, J., Zhao, L., 2018. A review of life cycle greenhouse gas (GHG) emissions of commonly used ex-situ soil treatment technologies. J. Clean. Prod. 186, 514–525.
Baldini, C., Bava, L., Zucali, M., Guarino, M., 2018. Milk production Life Cycle Assessment: a comparison between estimated and measured emission inventory for manure handling. Sci. Total Environ. 625, 209–219.
Braschel, N., Posch, A., 2013. A review of system boundaries of GHG emission inventories in waste management. J. Clean. Prod. 44, 30–38.
Briones Hidrovo, A., Uche, J., Martínez-Gracia, A., 2017. Accounting for GHG net reservoir emissions of hydropower in Ecuador. Renew. Energy 112, 209–221.
Cellura, M., Cusenza, M.A., Longo, S., 2018. Energy-related GHG emissions balances: IPCC versus LCA. Sci. Total Environ. 628-629, 1328–1339.
Coderoni, S., Esposti, R., 2018. CAP payments and agricultural GHG emissions in Italy. A farm-level assessment. Sci. Total Environ. 627, 427–437.
Hao, H., Geng, Y., Hang, W., 2016. GHG emissions from primary aluminum production in China: regional disparity and policy implications. Appl. Energy 166, 264–272.
Hu, Y., Yin, Z., Ma, J., Du, W., Liu, D., Sun, L., 2017. Determinants of GHG emissions for a municipal economy: structural decomposition analysis of Chongqing. Appl. Energy 196, 162–169.
Huang, W., Gao, Q.-X., G-L, Cao, Ma, Z.-Y., Zhang, W.-D., Chao, Q.-C., 2016. Effect of urban symbiosis development in China on GHG emissions reduction. Adv. Clim. Chang. Res. 7, 247–252.
IEA, 2018. Global Energy & CO2 Status Report 2017.
Johannes Friedrich, M.G., 2017. Andrew Pickens this Interactive Chart Explains World's Top 10 Emitters, and how They've Changed.
Kennedy, C., Steinberger, J., Gasson, B., Hansen, Y., Hillman, T., Havránek, M., et al., 2009. Greenhouse gas emissions from global cities. Environ. Sci. Technol. 43, 7297–7302.
Kroeze, C., Mosier, A., Nevison, C., Oenema, O., Seitzinger, S., Cleemput, et al., 1997. The Revised 1996 IPCC Guidelines for National Greenhouse Gas Inventories. Work 1–3.
La Notte, A., Tonin, S., Lucaroni, G., 2018. Assessing direct and indirect emissions of greenhouse gases in road transportation, taking into account the role of uncertainty in the emissions inventory. Environ. Impact Assess. Rev. 69, 82–93.
Leifeld, J., 2018. Distribution of nitrous oxide emissions from managed organic soils under different land uses estimated by the peat C/N ratio to improve national GHG inventories. Sci. Total Environ. 631-632, 23–26.
Li, Y., Du, W., Huisingh, D., 2017. Challenges in developing an inventory of greenhouse gas emissions of Chinese cities: a case study of Beijing. J. Clean. Prod. 161, 1051–1063.
Long, Y., Yoshida, Y., 2018. Quantifying city-scale emission responsibility based on input-output analysis – insight from Tokyo, Japan. Appl. Energy 218, 349–360.
Lou, Z., Cai, B.-F., Zhu, N., Zhao, Y., Geng, Y., Yu, B., et al., 2017. Greenhouse gas emission inventories from waste sector in China during 1949–2013 and its mitigation potential. J. Clean. Prod. 157, 118–124.
Marchi, M., Niccolucci, V., Pulselli, R.M., Marchettini, N., 2018. Environmental policies for GHG emissions reduction and energy transition in the medieval historic centre of Siena (Italy): the role of solar energy. J. Clean. Prod. 185, 829–840.

Montelongo-Reyes, M.M., Otazo-Sánchez, E.M., Romo-Gómez, C., Gordillo-Martínez, A.J., Galindo-Castillo, E., 2015. GHG and black carbon emission inventories from Mezquital Valley: the main energy provider for Mexico Megacity. Sci. Total Environ. 527-528, 455–464.
NDRC, 2004. The People's Republic of China Initial National Communication on Climate Change. China Planning Press.
Oehmichen, K., Thrän, D., 2017. Fostering renewable energy provision from manure in Germany – where to implement GHG emission reduction incentives. Energy Policy 110, 471–477.
Olivier, J.G.J., KMS, Peters, J.A.H.W., 2017. Trends in Global CO2 and Total Greenhouse Gas Emissions: 2017 Report. PBL Netherlands Environmental Assessment Agency, The Hague.
Park, S., Kim, H., Kim, B., Choi, D.G., 2018. Comprehensive analysis of GHG emission mitigation potentials from technology policy options in South Korea's transportation sector using a bottom-up energy system model. Transp. Res. Part D: Transp. Environ. 62, 268–282.
Penman, J., 2000. Good practice guidance and uncertainty management in national greenhouse gas inventories. D Cycleence & Management Kruger I Galbally T Hiraishi B Nyenzi, pp. 4.1–4.94.
Puliafito, S.E., Allende, D., Pinto, S., Castesana, P., 2015. High resolution inventory of GHG emissions of the road transport sector in Argentina. Atmos. Environ. 101, 303–311.
Qi, C., Wang, Q., Ma, X., Ye, L., Yang, D., Hong, J., 2018. Inventory, environmental impact, and economic burden of GHG emission at the city level: case study of Jinan, China. J. Clean. Prod. 192, 236–243.
Sanna, L., Ferrara, R., Zara, P., Duce, P., 2014. GHG emissions inventory at urban scale: the Sassari case study. Energy Procedia 59, 344–350.
Song, Q., Wang, Z., Wu, Y., Li, J., Yu, D., Duan, H., et al., 2018a. Could urban electric public bus really reduce the GHG emissions: a case study in Macau? J. Clean. Prod. 172, 2133–2142.
Song, X., Zhang, C., Yuan, W., Yang, D., 2018b. Life-cycle energy use and GHG emissions of waste television treatment system in China. Resour. Conserv. Recycl. 128, 470–478.
Sówka, I., Bezyk, Y., 2018. Greenhouse gas emission accounting at urban level: a case study of the city of Wroclaw (Poland). Atmos. Pollut. Res. 9, 289–298.
Talbot, D., Boiral, O., 2013. Can we trust corporates GHG inventories? An investigation among Canada's large final emitters. Energy Policy 63, 1075–1085.
Tanaka, K., O'Neill, B.C., 2018. The Paris Agreement zero-emissions goal is not always consistent with the 1.5 °C and 2 °C temperature targets. Nat. Clim. Chang. 8, 1–6.
Tayarani, M., Poorfakhraei, A., Nadafianshahamabadi, R., Rowangould, G., 2018. Can regional transportation and land-use planning achieve deep reductions in GHG emissions from vehicles? Transp. Res. Part D: Transp. Environ. 63, 222–235.
UNFCCC, 2018. https://unfccc.int/process/the-paris-agreement/what-is-the-paris-agreement.
Villalba, G., Gemechu, E.D., 2011. Estimating GHG emissions of marine ports—the case of Barcelona. Energy Policy 39, 1363–1368.
Wang, S., Liu, X., 2017. China's city-level energy-related CO2 emissions: spatiotemporal patterns and driving forces. Appl. Energy 200, 204–214.
Wiik, M.K., Fufa, S.M., Kristjansdottir, T., Andresen, I., 2018. Lessons learnt from embodied GHG emission calculations in zero emission buildings (ZEBs) from the Norwegian ZEB research centre. Energ. Buildings 165, 25–34.
Xi, F., Geng, Y., Chen, X., Zhang, Y., Wang, X., Xue, B., et al., 2011. Contributing to local policy making on GHG emission reduction through inventorying and attribution: a case study of Shenyang, China. Energy Policy 39, 5999–6010.
Xu, X., Zhao, T., Liu, N., Kang, J., 2014. Changes of energy-related GHG emissions in China: an empirical analysis from sectoral perspective. Appl. Energy 132, 298–307.
Yue, W., Cai, Y., Su, M., Yang, Z., Dang, Z., 2018. A hybrid copula and life cycle analysis approach for evaluating violation risks of GHG emission targets in food production under urbanization. J. Clean. Prod. 190, 655–665.
Zeng, Y., Tan, X., Gu, B., Wang, Y., Xu, B., 2016. Greenhouse gas emissions of motor vehicles in Chinese cities and the implication for China's mitigation targets. Appl. Energy 184, 1016–1025.
Zhang, G., Ge, R., Lin, T., Ye, H., Li, X., Huang, N., 2018. Spatial apportionment of urban greenhouse gas emission inventory and its implications for urban planning: a case study of Xiamen, China. Ecol. Indic. 85, 644–656.